MEASUREMENTS OF THE SECONDARY ELECTRON EMISSION FROM DIELECTRIC SURFACES

by

ELISE R. BOERWINKLE, B.S. in Eng. Phys.

A THESIS

IN

PHYSICS

Submitted to the Graduate Faculty
of Texas Tech University in
Partial Fulfillment of
the Requirements for
the Degree of

MASTER OF SCIENCE

Approved

Accepted

December, 1988

TABLE OF CONTENTS

LIST OF FIGURES

CHAPTER I

INTRODUCTION

Secondary electron emission from dielectrics is an area of active research. Knowing the secondary electron emission curves for dielectrics will help us better understand the way these materials function in different situations. This basic information may allow scientists to develop more accurate models for the behavior of these materials. For instance, Burke,[1] states that secondary electron emission (SEE) curves are required to model charge build-up on spacecrafts. This is an important problem, because it is difficult to ground an object orbiting in space.

Surface flashover of polymers is another area in which the SEE plays an important role. At Texas Tech University, Leiker[2] has applied a hydrocarbon coating to a variety of materials, and tested the resulting flashover voltage. The coating is formed by placing a disk-shaped sample between two electrodes and rotating it about its central axis in a vacuum. While the sample is rotating, a jet airplane engine sparkplug is sparked repeatedly in the vacuum, and a coating forms on the sample. Then the electrodes are used to stress the sample electrically until flashover occurs. Other current work at Texas Tech University involves computer modeling of surface flashover. This modeling work requires data from SEE measurements for both virgin, uncoated polymers, and the treated, or coated polymers.

When a primary electron strikes a surface, part or all of its energy may be transferred to an atom in the lattice of the material and an electron may be emitted. This emitted electron is called a secondary electron or just a "secondary." The ratio of the number of secondaries leaving

---

[1]E. A. Burke, "Secondary Emission from Polymers," IEEE Transactions on Nuclear Science *NS-27* (1980), pp. 1760-1764.

[2]G. R. Leiker, Ph.D. Dissertation, Texas Tech University, 1988.

the surface to the number of primary electrons striking the surface is known as the secondary electron emission coefficient, δ.

There are three ways electrons can leave a surface that is struck by an electron beam. Part of the primary beam may be elastically reflected, part of it may be inelastically reflected, and part of it may interact with the material to form secondary electrons. The electrons leaving the material may be elastically or inelastically scattered primaries or they may be true secondaries. The term "true secondaries" usually refers to all those electrons with an energy below about 50 eV.[3]

The ratio of the total number of electrons leaving the surface to the number of primaries incident on the surface is the total yield, σ. The ratio of the number of elastically and inelastically reflected primaries leaving the surface to the number of incident primaries is the backscattered yield, η. The total yield, σ, is made up of the true secondaries, δ, and the reflected primaries, η:

$$\sigma = \delta + \eta. \tag{1.1}$$

For low energy electrons bombarding polymers, the number of reflected electrons is much lower than the number of secondaries, so δ, the secondary electron emission coefficient (SEEC), is very close to the total yield, σ. We use the approximation that $\delta = \sigma$.[4]

It is known from previous studies[5] that the δ of a material is a function of the energy of the incident electrons and of the material itself. In Figure 1.1, the points $E_{0.1}$ and $E_{0.2}$ are called the crossover points because they are the energies at which δ is equal to one. At $\delta = 1$ the number of secondary electrons leaving the surface is the same as the number of primaries which strike it.

---

[3]A. J. Dekker, *Solid State Physics* (Englewood Cliffs, N. J.: Prentice-Hall, 1957), p. 420.

[4]H. von Seggern, "Charging Dynamics of Dielectrics Irradiated by Low-Energy Electrons," IEEE Transactions on Nuclear Science *NS-32* (1985), pp. 1503-1511.

[5]H. Bruining, *Physics and Applications of Secondary Electron Emission* (New York: McGraw-Hill, 1954) and A. J. Dekker, "Secondary Electron Emission," Solid State Physics *6* (1958), pp. 251-311.

When δ is greater than one, more secondaries leave the material than the number of primaries which strike it and the surface charges positively; when δ is less than one, there are fewer secondaries leaving than incoming primaries and the surface charges negatively.

The maximum value of δ is labeled δ_m and the corresponding value of incident energy is called $E_{0,m}$. These quantities can be used to compare δ vs. E_0 curves for different materials.

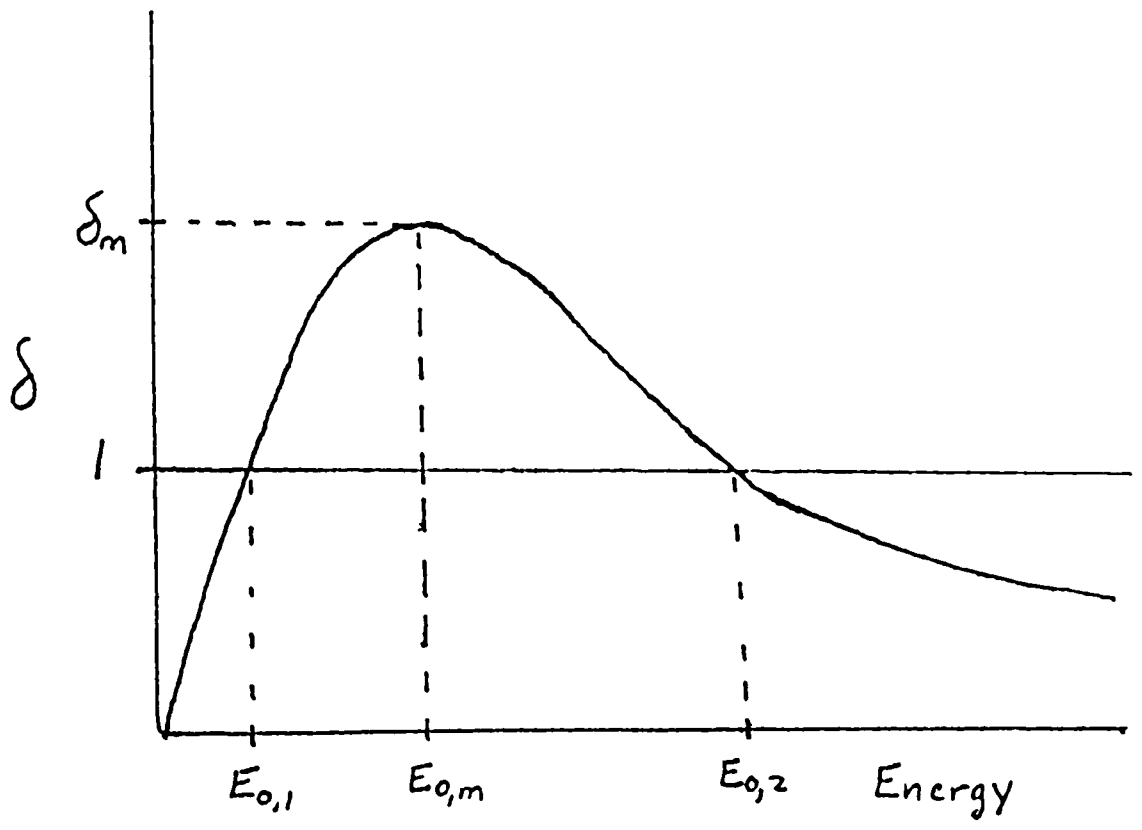

Figure 1.1: Typical δ vs. Energy Curve

CHAPTER II

THEORY

There are two stages in the process of secondary electron emission, as the elementary theory is given by A. J. Dekker.[1] The actual production of secondaries is the first stage. The second stage deals with the probability that the secondaries produced will escape from the surface. The secondary yield, δ, can be expressed as a function of the number of secondaries $n(x)$ produced by one primary between the depths x and $x + dx$, and the probability $f(x)$ for the secondary to migrate and escape from the surface,

$$\delta = \int n(x) f(x) dx, \tag{2.1}$$

where the integral is taken over the total thickness of the sample. There are five basic assumptions which are used in this elementary theory:

- The primaries move in a straight line along the direction of incidence after they enter the solid; this neglects all scattering of the primaries (both elastic and inelastic).
- The primary beam is incident perpendicular to the surface.
- The primaries' energy loss per unit length is described by Whiddington's law

  $$-\frac{dE_p(x)}{dx} = \frac{A}{E_p(x)},$$

  where $E_p(x)$ is the energy of the primary, and A is a constant of the material.
- A single primary can produce $n(x)$ secondaries in a layer of thickness dx:

  $$n(x) = -\frac{1}{\epsilon_e}\frac{dE_p}{dx},$$

  where ϵ_e is the average excitation energy required to produce a secondary inside the solid.

[1] Dekker, (1957), p. 423.

- A secondary produced at a depth, x, has a probability, $f(x)$, of escape from the surface that follows an exponential absorption law,

$$f(x) = f(0)e^{(-x/x_s)},$$

where $f(0)$ is the escape probability near the surface, and x_s is the range of the secondaries in the material.

So Dekker[2] writes:

$$\delta = -\frac{B}{\epsilon}\int \frac{dE}{dx}e^{\alpha x}dx, \tag{2.2}$$

where $B = f(0)$ and $\alpha = -\frac{1}{x_s}$. This is not a complete description of secondary electron emission, but a semiempirical theory. It makes three oversimplifying assumptions:

- It assumes that there is a clear-cut distinction between the production mechanism and the escape mechanism.

- It does not consider the energy distribution of the secondaries, only the number of secondaries.

- The escape mechanism is described by an exponential absorption law without regard to the physical processes involved.

This theory cannot be used to predict the yield for a particular material, but it can be used to suggest a general shape for the yield curves.

Burke[3] shows that Dekker's semiempirical model of secondary electron emission predicts a power function dependence of the high energy yield on energy. Burke found that

$$\delta = KE_0^{-n}, \tag{2.3}$$

with E_0 in keV. The yield coefficient K is given by

$$K = 12.1E_{0,m}^{1.725} \tag{2.4}$$

---

[2]Dekker, (1958).
[3]Burke.

for polymers. With this equation, it is possible to estimate the yield curve if two of the three parameters δ_m, $E_{0.m}$, or K are known. Burke finds the best fit for polymers to have $n = 0.725$. We will compare this to our data later.

Dekker[4] states that yield curves for all materials exhibit the same general shape, apart from quantitative differences. The SEEC rises to a peak, δ_m, at some $E_{0.m}$, then falls off with increasing energy. Baroody[5] was the first to plot $\frac{\delta}{\delta_m}$ vs. $\frac{E}{E_{0.m}}$, and show that data points for a large number of materials fall within a narrow region. This type of curve is called a universal curve. All universal curves have a maximum at the same point, ($\frac{\delta}{\delta_m} = 1, \frac{E}{E_{0.m}} = 1$), so the shapes of the curves can easily be compared. The right side of a universal curve is different for polymers and metals.

Several experimental studies have been done on polymers, some on thin films, some on bulk materials. It was expected that thin films may have different SEE curves than bulk samples because of the amorphous nature of the films.[6] In Kazantsev and Matskevich's study of polymethyl methacrylate at 25 keV,[7] they showed the secondary electron emission curve from Matskevich's earlier work,[8] Figure 2.1. Matskevich and Mikhailova[9] compared their data on ice and anthracene with Matskevich's data on polyethylene and polystyrene[10] and Bruining's carbon data,[11] Figure 2.2. They used carbon to show how dielectrics' yield curves differed from the yield curve of a conductor. They show δ_m's from 1.3 to 2.3, and $E_{0.1} < 100$ eV for dielectrics.

---

[4]Dekker, (1957), p. 421.

[5]E. M. Baroody, "A Theory of Secondary Electron Emission from Metals," Physical Review *78* (1950), pp. 780-787.

[6]N. R. Whetten, "Secondary Electron Emission of Vacuum-Cleaved Solids," Journal of Vacuum Science & Technology, *2* (1965), pp. 84-86.

[7]A. P. Kazantsev and T. L. Matskevich, "Secondary Electron Emission of Methylmethacrylate at 25 keV," Soviet Physics-Solid State *6* (1965), pp. 1898-1904.

[8]T. L. Matskevich, "Secondary Electron Emission of Some Polymers," Fizika Tverdogo Tela, Collected Papers, *1* (1959), pp. 277-279.

[9]T. L. Matskevich and E. G. Mikhailova, "Secondary Electron Emission in Ice and Anthracene Films," Soviet Physics-Solid State *2* (1960), pp. 655-659.

[10]Matskevich.

[11]Bruining.

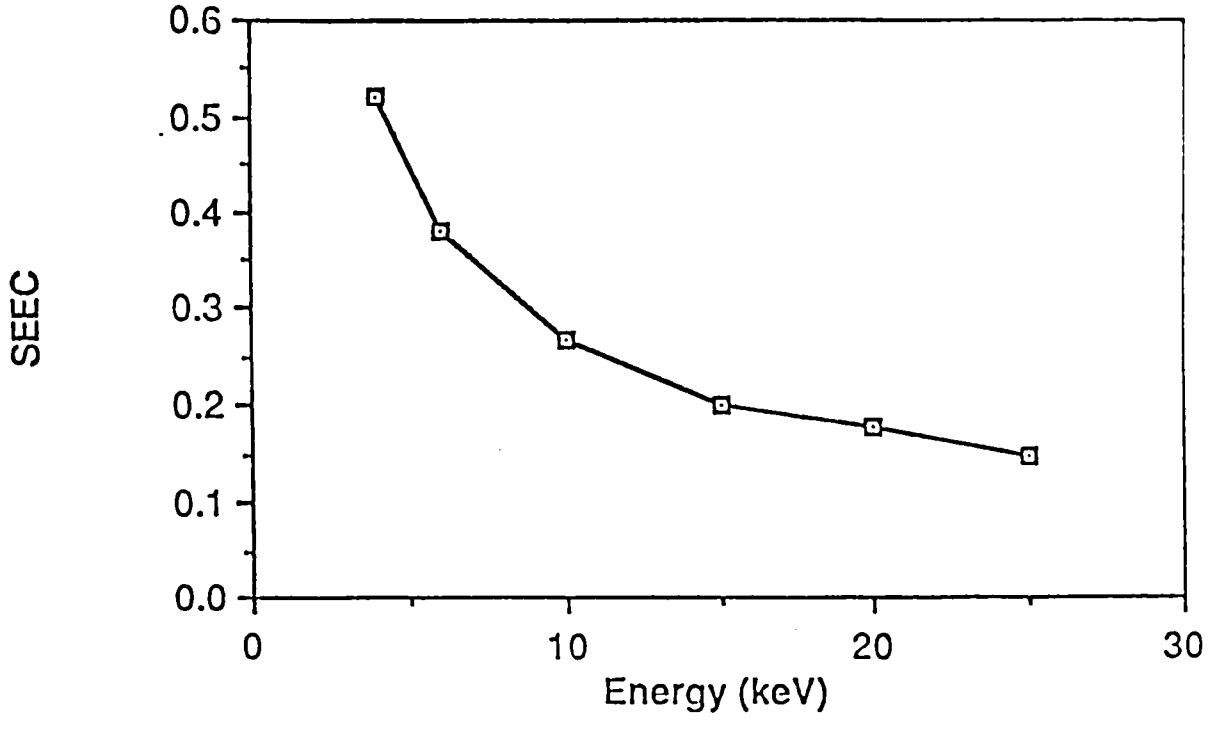

Figure 2.1: Methylmethacrylate SEE Data from Kazantsev and Matskevich.

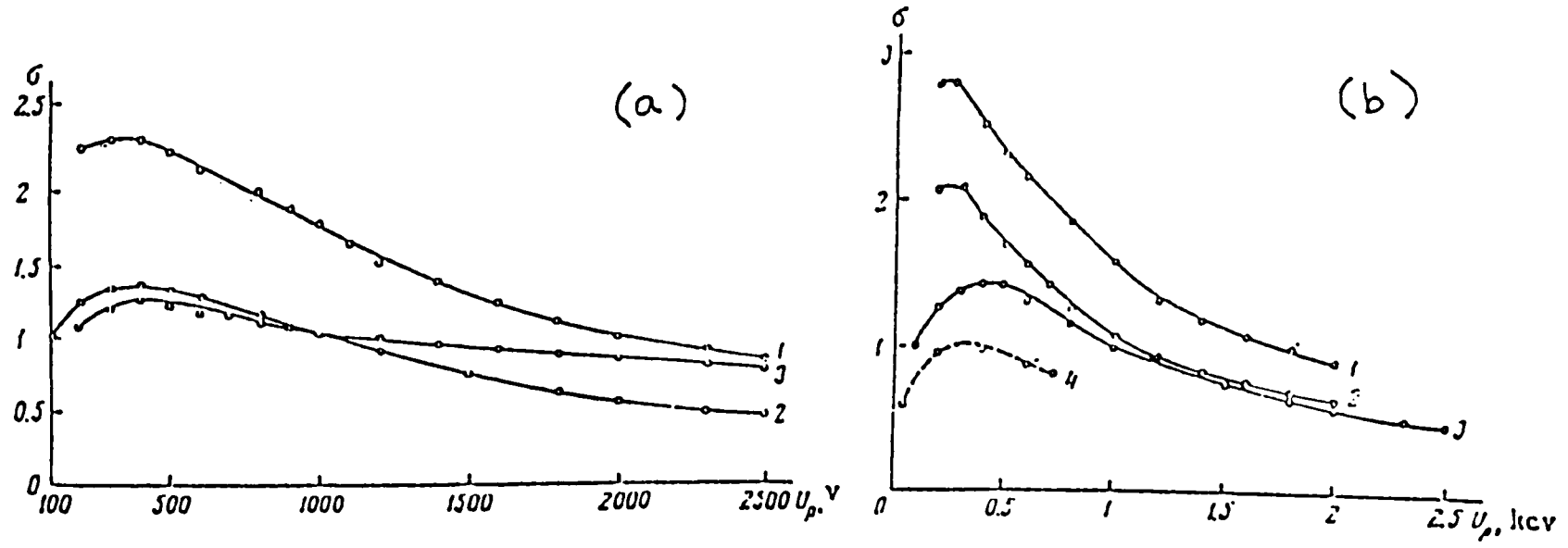

Figure 2.2: SEE Data from Matskevich and Mikhailova. (a) 1) ice; 2) anthracene; 3) molybdenum. (b) 1) polyethylene (Matskevich); 2) polystyrene (Matskevich); 3) anthracene; 4) carbon (Bruining).

Burke[12] also quoted Matskevich when plotting experimental data on his universal curve for polymers, Figure 2.3. Willis and Skinner's[13] total yield for four polymers from .05 to 2.5 keV and their universal curve are shown in Figure 2.4. They show $E_{0.1}$'s of from $20 - 50$ eV and δ_m's from 2.1 to 4.8. All of the preceeding work was done on films of the polymers, but Gross, von Seggern, and Berraissoul[14] presented data on bulk samples of four polymers and also plotted their data on a universal curve, Figure 2.5. Their curves show $E_{0.1} < 100$ eV for all of their polymers and δ_m's range from 1.8 to 2.0.

---

[12]Burke.

[13]R. F. Willis and D. K. Skinner, "Secondary Electron Emission Yield Behavior of Polymers," Solid State Communications *13* (1973), pp. 686-688.

[14]B. Gross, H. von Seggern, and A. Berraissoul, "Surface Charging of Dielectrics by Secondary Emission and the Determination of Emission Yield," IEEE Transactions on Electrical Insulation *EI-22* (1987), pp. 23-28.

Figure 2.3: Burke's Universal Curve

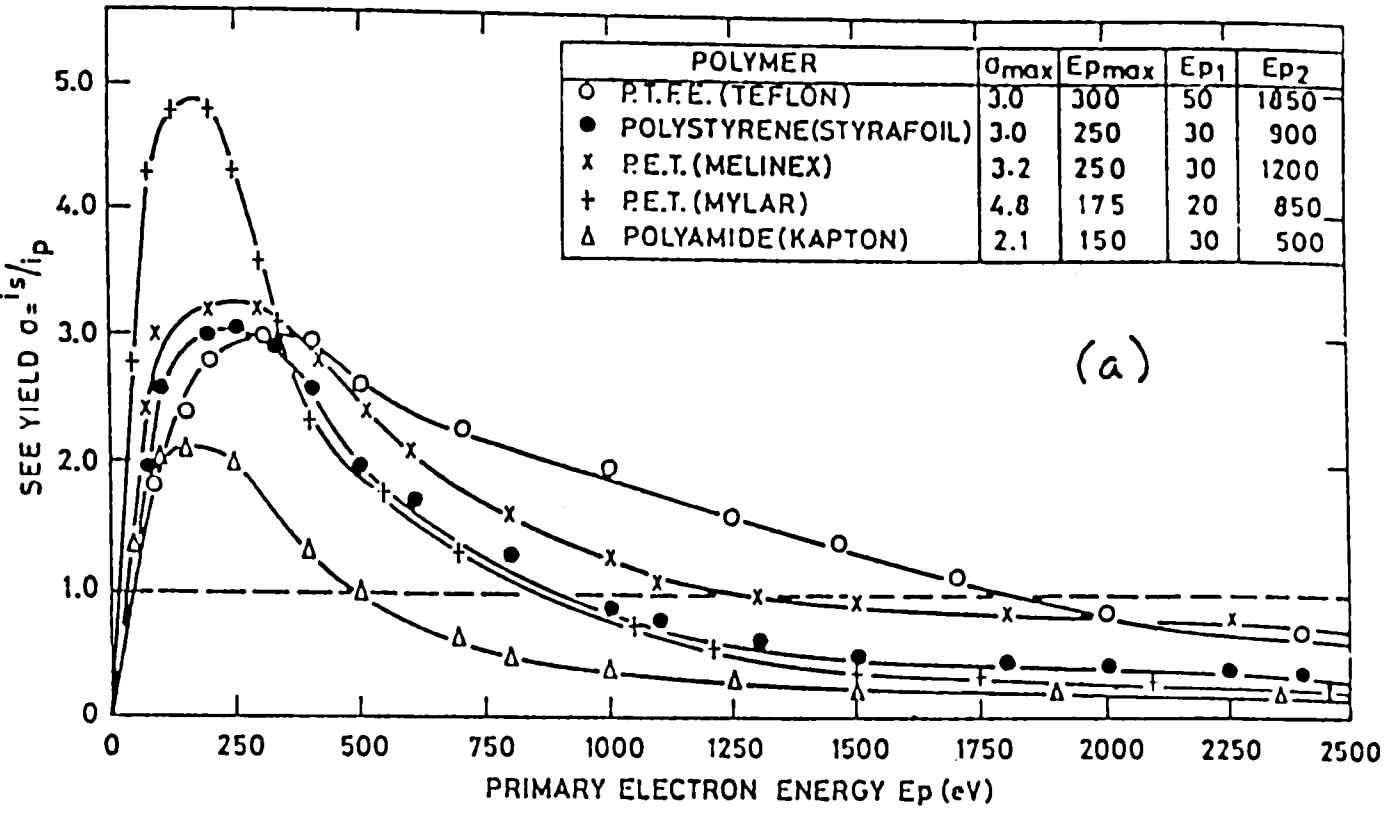

Figure 2.4: Willis and Skinner's Yield Curve (a) and Universal Curve (b).

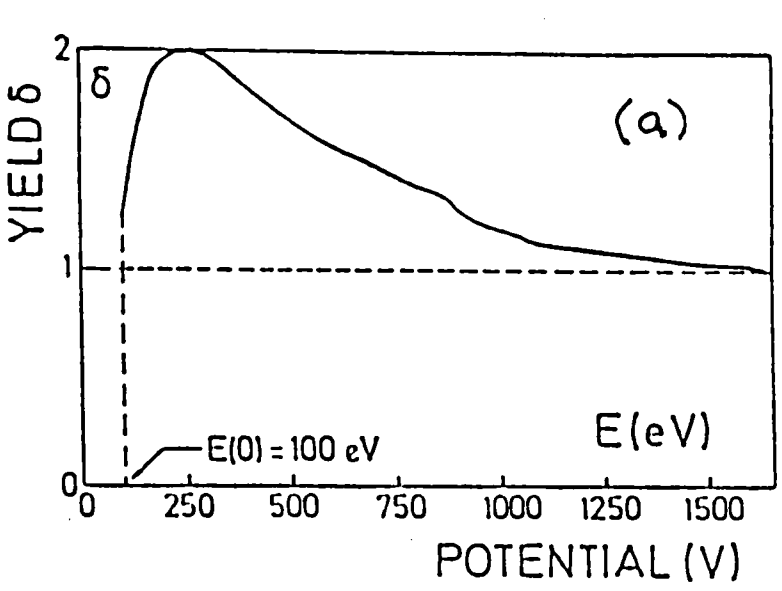

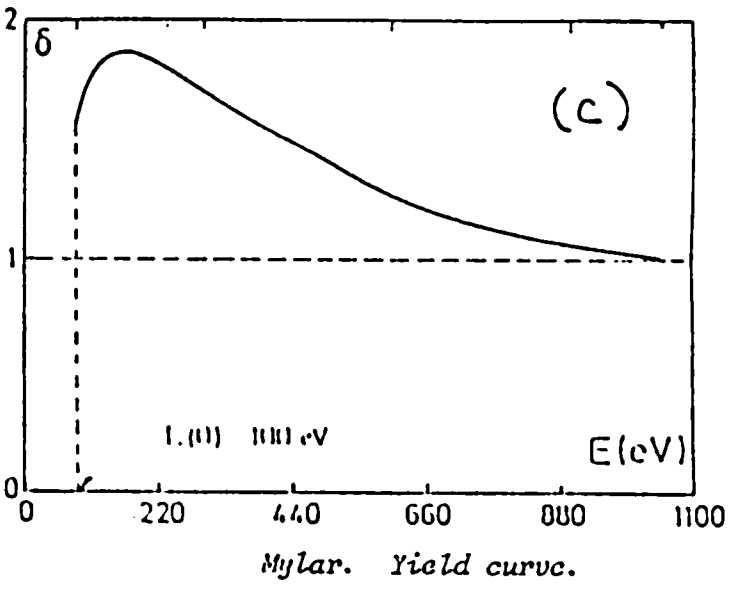

Mylar. Yield curve.

Aclar. Yield curve.

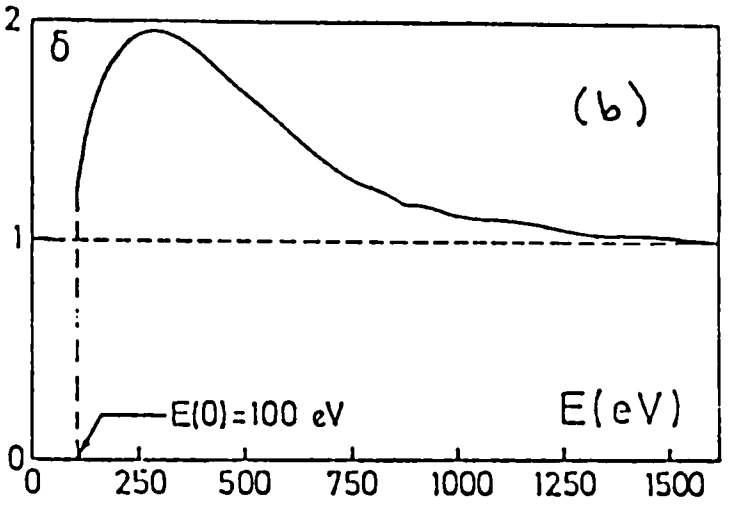

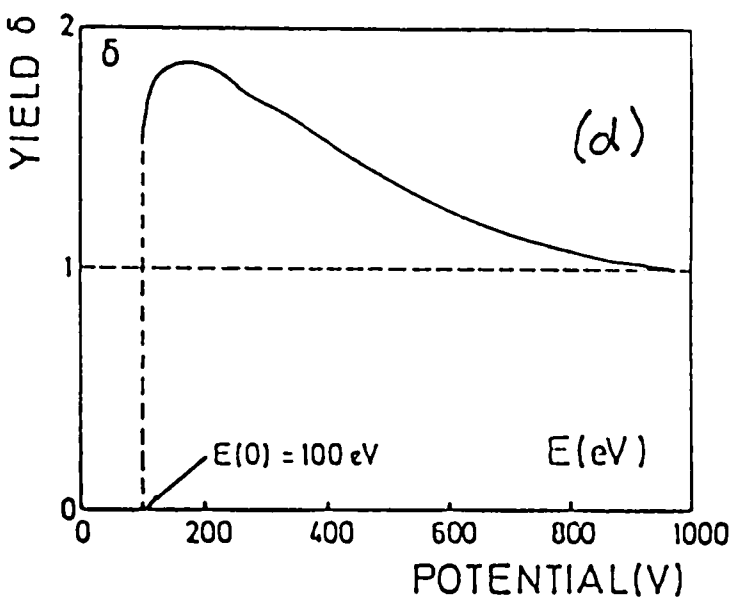

Teflon. Yield curve.

Kapton. Yield curve.

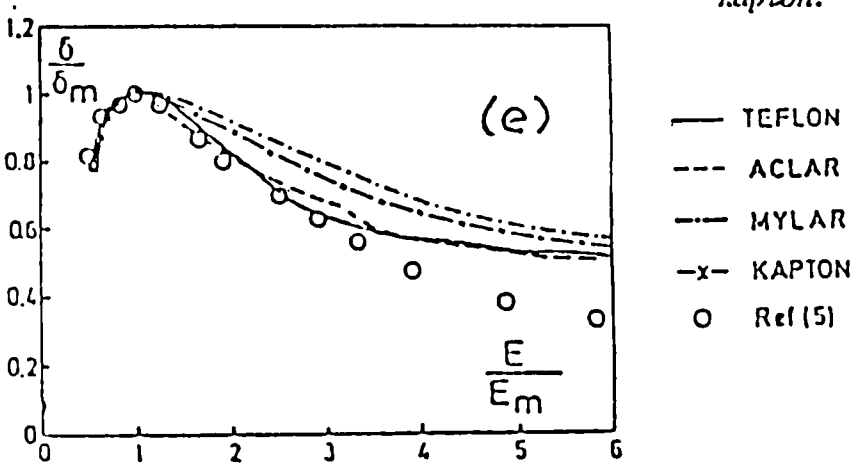

Universal curve.

Figure 2.5: Gross, von Seggern, and Berraissoul's Yield Curves (a)-(d) and Universal Curve (e).

CHAPTER III

METHOD

To find SEEC curves for dielectrics, we use a recently published method developed just for dielectrics. Based on the work of Gross, von Seggern, and Berraissoul,[1] the dielectric sample is treated as a parallel plate capacitor. The top surface of the sample is left electrically floating, and the bottom surface is metallized and connected to ground or a negative potential. The replacement current, I_0, results from the difference between beam current (the current due to the electron beam) and the secondary current (due to the secondaries leaving the surface,)

$$I_0 = I_b - I_s. \tag{3.1}$$

The surface potential, V_s, and the replacement current to the sample, I_0, are measured to determine δ of the sample material.

We start with a negatively biased sample in a grounded chamber, then irradiate the sample with electrons of potential just a few volts more negative. If the incident electrons have an effective energy above the first crossover point but below the second, then the surface will emit more electrons then it receives because δ is greater than one, so the surface will charge positively until it reaches zero potential with respect to the chamber walls. All of the secondaries created in this region will be emitted, because the sample surface is still negative with respect to the chamber walls, until the potential difference reaches zero, so the secondaries are repelled from the sample. Once the surface voltage does get to zero, if it then becomes positive, all the

[1]Gross, von Seggern, and Berraissoul.

secondaries will be recalled, forcing the voltage back to zero. This is the "self-regulating mechanism" described in the paper by Gross, von Seggern, and West.[2]

Our goal is to determine how the secondary electron emission coefficient varies as a function of the effective incident energy E_0. The SEE coefficient, δ, is defined as the ratio of the number of liberated secondaries to the number of incident primaries:

$$\delta = \frac{I_s}{I_b}. \tag{3.2}$$

We apply a known voltage, $-V_0$, to the bottom of the sample, as shown in Figure 3.1. (The figure shows conventional current, not electron current.) The initial effective energy of the primaries which strike the sample will be:

$$E_0 = E_b - eV_0$$

where E_b is the beam energy. (We use $eV_0 < E_b$). Because the sample is a dielectric the surface will begin to charge if the energy of the incident electrons is not exactly the energy of one of the crossover points. If the initial effective energy of the beam is less than the first crossover point,

$$E_b - eV_0 < E_{0.1},$$

then $\delta < 1$ (fewer secondaries emitted than primaries incident),[3] and the surface will charge negatively. ThBe negative surface then repels the incoming electrons. If the initial effective energy of the beam is between the first and second crossover points,

$$E_{0,1} < E_b - eV_0 < E_{0.2},$$

---

[2]B. Gross, H. von Seggern, and J. E. West, "Positive Charging of Fluorinated Ethylene Propylene Copolymer (Teflon) by Irradiation with Low-energy Electrons," Journal of Applied Physics *56* (1984), pp. 2333-2336.

[3]Whetten.

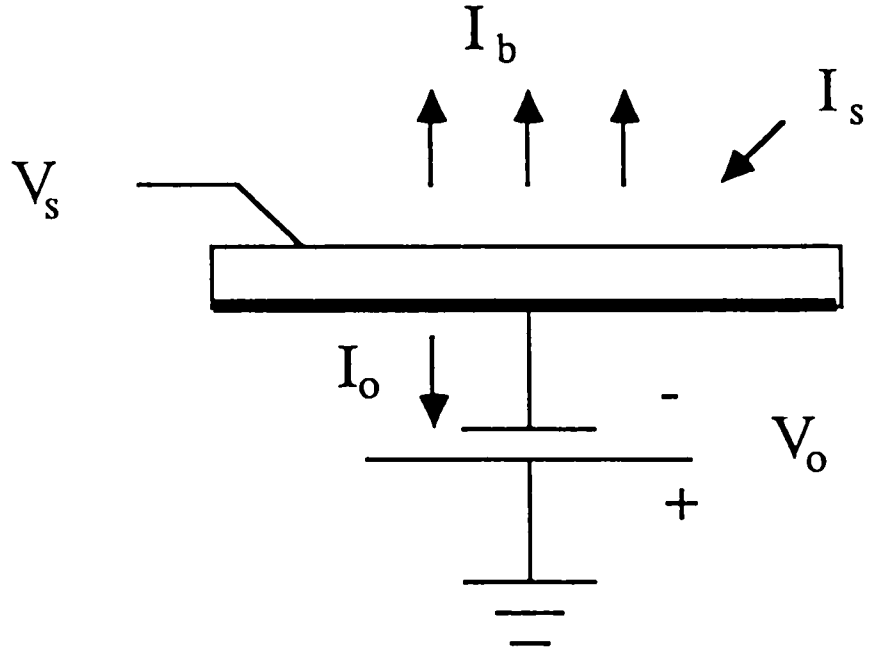

Figure 3.1: Schematic of Sample as Parallel Plate Capacitor

$\delta > 1$ (more secondaries than primaries), and the surface charges positively. As the surface charges positively, the effective energy of the incident electrons, E_0, increases. To find E_0, we need to know the actual surface potential, V_s:

$$V_s = V_0 + \Delta V_s.$$

We get the change in V_s from our treatment of the sample as a parallel plate capacitor. The potential across a parallel plate capacitor is given by

$$V = \frac{Q}{C},$$

where Q is the charge on the capacitor and C is the capacitance. For our samples, the change in potential of the surface is given by:

$$\Delta V_s = \frac{\Delta Q}{C}. \tag{3.3}$$

If the leakage current can be neglected, as we assume, then the following is true:

$$I_0 = C\frac{dV_s}{dt} \tag{3.4}$$

$$\Delta V_s = \frac{1}{C}\int I_0 dt, \tag{3.5}$$

where V_s is the surface voltage. The incident electron energy becomes:

$$E_0 = E_b - eV_0 + e\Delta V_s \tag{3.6}$$

or, using Eqn. (3.5),

$$E_0 = E_b - eV_0 + \frac{e}{C}\int I_0 dt. \tag{3.7}$$

Our expression for E_0 shows that the incident electron energy is a function of time. We need to find the replacement current, I_0, as a function of time. To do this, we connect an electrometer to the metallized bottom of the sample, and measure the replacement current which enters the sample from the bottom. The electrometer feeds the signal to a chart recorder, which plots

replacement current, I_0, vs. time. This allows us to find E_0 at any given time. We can then use Eqn. (3.1) and Eqn. (3.2) to get one equation relating the beam current, I_b (known), and the replacement current, I_0 (measured), to the SEE coefficient, δ;

$$\delta = \frac{I_b - I_0}{I_b}. \tag{3.8}$$

We now have both δ and E_0 as functions of time, so at chosen points in time we can plot δ vs. E_0. This gives us what we were looking for: the secondary electron emission curve as a function of incident electron energy.

CHAPTER IV

EXPERIMENTAL SETUP

To use the method described in the previous chapter, we have a vacuum system with three chambers, as shown in Figure 4.1: the main pumping chamber, the sample chamber, and the electron gun chamber. The basic setup was built by Mary Baker,[1] but it has undergone some modifications. The main pumping chamber has a pumping stack consisting of a mechanical pump, a diffusion pump, and a cold trap. The Sargent Welch model 1397 mechanical pump is connected through a valve to the four-inch diffusion pump and is filled with Santovac 5, a five-ring polyphenylether fluid. The Varian 362-4 Cryotrap is filled with methyl alcohol. A Neslab CC-65A cryocool immersion cooler with an extra long probe cools the methyl alcohol to -60 C, under no-load conditions. The foreline pressure of the diffusion pump can be measured with a thermocouple hooked to a Veeco TG-7 thermocouple gauge control. Another thermocouple connected to the same controller gives the pressure above the diffusion pump. This chamber has a valve on top to let in dry nitrogen, so that less water vapor and contaminants get into the chamber during sample change-out, and the next pumping time is reduced.

The sample chamber is separated from the main pumping chamber by a Varian six-inch electropneumatic swing gate valve. All seals in the sample chamber are O-ring type seals. To pump down this chamber, a Duo Seal model 1405 small mechanical pump with a foreline molecular sieve trap is connected to the chamber via a bellows valve. After the chamber is rough pumped down to a pressure below 100 mTorr, the six-inch gate valve is opened and the pumping stack brings the pressure down further. For pressures above 10 mTorr, pressure readings are taken from the Veeco thermocouple controller that was used for the main pumping chamber. At

[1]M. C. Baker, Master's Thesis, Texas Tech University, 1985.

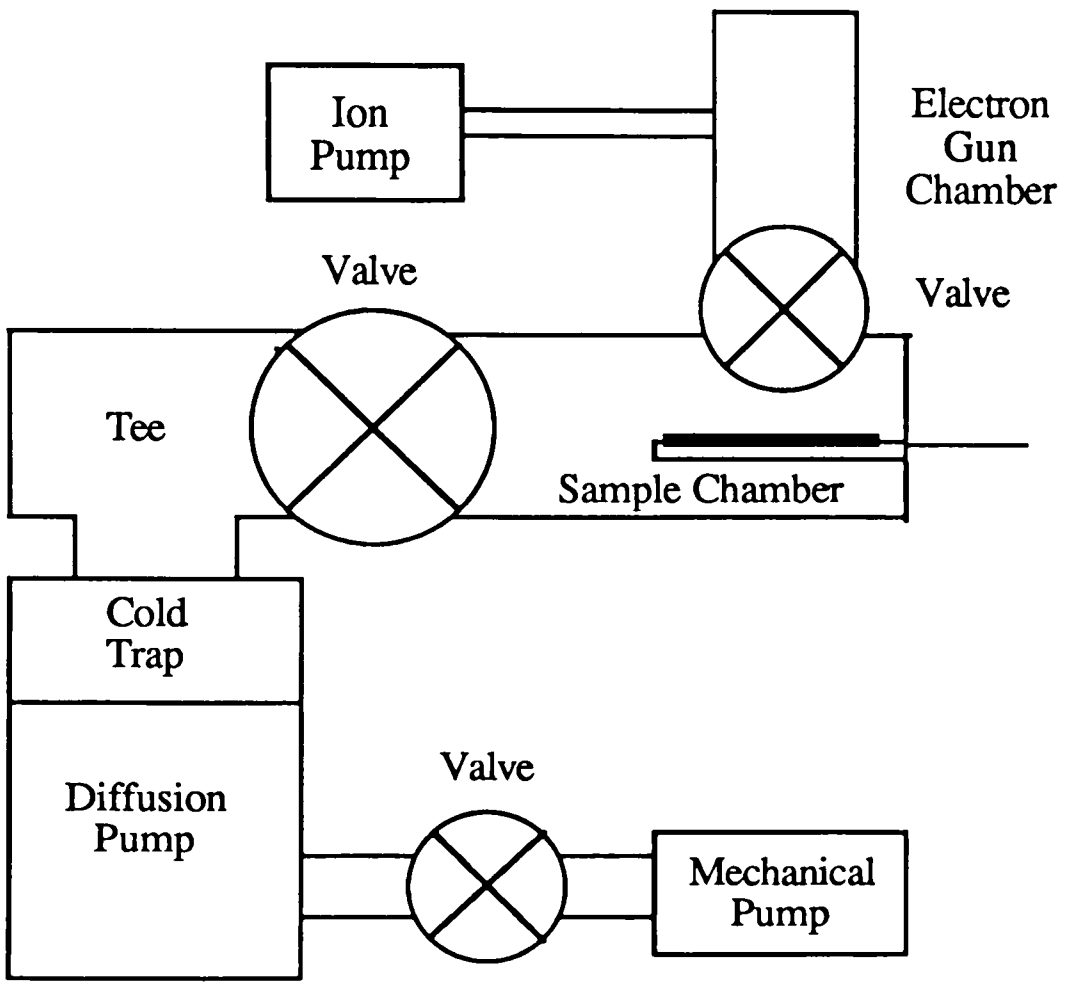

Figure 4.1: Block Diagram of the Vacuum System

lower pressures, a Granville Phillips Ionization Gauge Controller and an ion gauge tube with a thoria coated iridium filament measure the pressure. At the bottom of the sample chamber there is an electrical feedthrough for connection to the bottom of the sample.

The sample chamber contains the sample holder, which consists of a Lucite slide and an aluminum guide track, shown in Figure 4.2. The slide moves horizontally along the guide track by means of a linear motion feedthrough in the wall of the vacuum chamber. The Lucite slide holds six sample sites. Each sample site has a circular aluminum plate, one centimeter in diameter, which is held to the Lucite by a small brass bolt which passes through the plate and the Lucite slide. A dovetail notch is cut on the bottom of the slide and a matching dovetail groove is cut on the top of the guide track, so they fit together smoothly. The aluminum guide track has a Teflon cylindrical insert with a bolt through it. At the top of this bolt, there is a metal spring finger which is depressed by the smaller bolt through the Lucite at one of the sample sites when a sample is in position. This makes the necessary electrical contact. The bottom of the bolt in the Teflon connects to a wire which goes to the electrical feedthrough at the bottom of the sample chamber.

The first sample position is used for the calibration sample. We use a disk of pure graphite, one centimeter in diameter. The replacement current to the graphite is measured by the electrometer, and then we use the SEE curve for graphite found in Bruining's book[2] to calculate the beam current, I_b. We assume that the beam current stays constant during a single sample run. The current is checked on the graphite before and after each run. When there is a large change in replacement current to the graphite, the acquired data are discarded.

The second sample site holds a fluorescent chip, a little larger than a sample. This chip is part of an old cathode ray tube (CRT) screen. This small screen allows us to center the electron beam on the sample, and shows us the shape and size of the beam.

---

[2] Bruining.

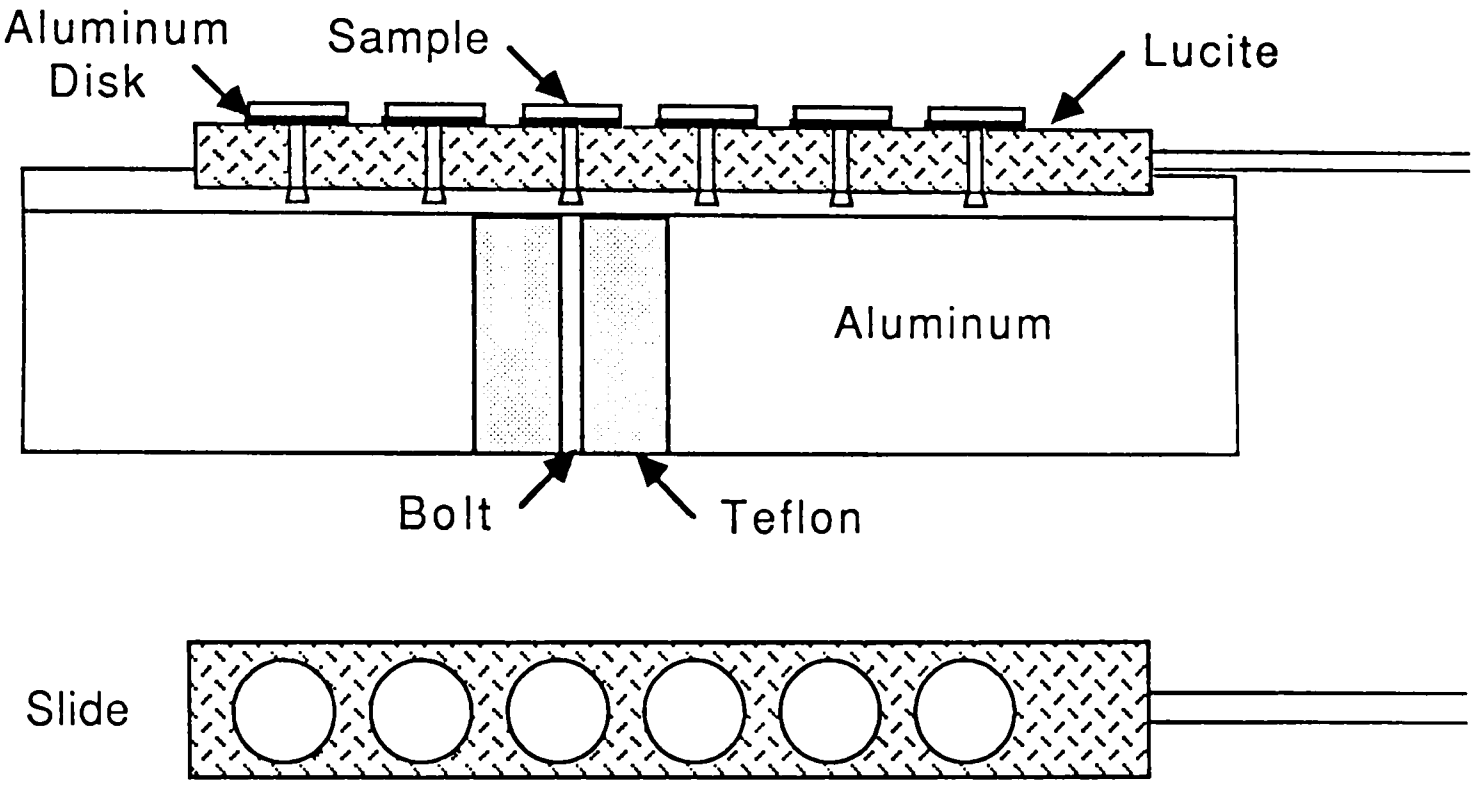

Figure 4.2: Sample Holder showing Slide and Places for 6 Samples

The dielectric samples we use are taken from three-inch diameter, commercially available rods. A slice about one inch thick is cut from the end of a rod, then a lathe is used to cut a smaller rod of one centimeter diameter along a diameter of the slice. One end of this smaller rod is polished, first with Crest regular toothpaste, then rinsed with water and polished with powdered alumina (1 micron grit) and water. The rod is then placed in an Isomet slow speed saw with a diamond blade, and a sample about one millimeter thick is cut off. This sample is washed with cyclohexane to remove any contaminants from the polishing. The cut, unpolished sides of some samples are coated by vacuum evaporated Al. The aluminum backed samples are then attached to a sample site using a small drop of silver colloidal paint. The samples that do not have aluminum backings are painted with a thin, even layer of the silver paint, then placed on a sample site. (There is no difference in SEEC curves for the two ways the samples are attached.)

The electron gun chamber is separated from the sample chamber by a three-inch gate valve, which can be pneumatically closed, but must be manually opened. Just above this valve is a metal plate with a small hole in the center. This plate serves to keep the higher pressure in the sample chamber from greatly affecting the pressure in the top chamber. The top chamber has two multi-pin electrical feedthroughs for the wires of the electron gun inside. The electron gun chamber is pumped by a Perkin Elmer model 203-2500, 25 l/s, ion pump at the end of a long, two-inch diameter, pipe.

The electron gun is made from an RCA 3JP1 oscillograph tube, a cathode ray tube (CRT). This CRT previously had the fluorescent screen cut off the bottom end, and had been used as an electron gun until the cathode cup was poisoned. To replace the cathode cup, the top of the CRT was removed by running a current through a nichrome wire wrapped tightly around the outside of the glass tube, in a track scored by a file. By rapidly heating and cooling the wire through controlling the current, the glass was broken along the scored line. We removed the used cathode cup and installed a thoriated tungsten filament of the type used in a scanning electron

microscope (SEM). The wires to the top of the gun were spot welded to longer wires to connect to the vacuum feedthroughs on top of the chamber.

The electron beam is aimed vertically down, and must pass through a hole in the mask. The mask is a metal support for the gun, electrically isolated from the rest of the chamber. For initial steering of the electron beam, a picoammeter was connected to the mask to find when the beam went through the hole. The beam must also pass through the hole in the metal plate separating the gun chamber from the sample chamber if it is to strike the sample.

There are several electronic systems to control the experiment (see Figure 4.3). Potentiometers control the potential applied to the deflection plates which steer the electron beam. The beam is focused through the use of the anode in the original structure of the CRT. The two orthogonal sets of deflection plates are supplied with voltage by two identical DC power supplies. A separate circuit delivers high voltage from a 2000 volt Fluke high voltage DC power supply to the grid, and from there to the anode and cathode. The anode focuses the beam, and the potentiometer connected to the grid controls the electron beam current by regulating the difference in potential between the cathode and the grid. There is a switch and a Variac to control the heating of the cathode. A light indicates when the filament has current running through it. All of these electronic controls are located together in one rack-mounted component for easy access and operation.

The earth's magnetic field is strong enough to deflect the electron beam. There are three sets of orthogonal Helmholtz coils surrounding the electron gun and the sample chamber to counteract most of the earth's magnetic field. Each coil is made of fifty turns of wire, and has a separate current regulator to control the amount of current in the coil.

The high voltage feedthrough at the bottom of the sample chamber electrically connects the sample to be tested to the current measuring circuit. The dielectric sample is attached to three photographic flash batteries (nominally 510 volts each) to set its initial potential, through the

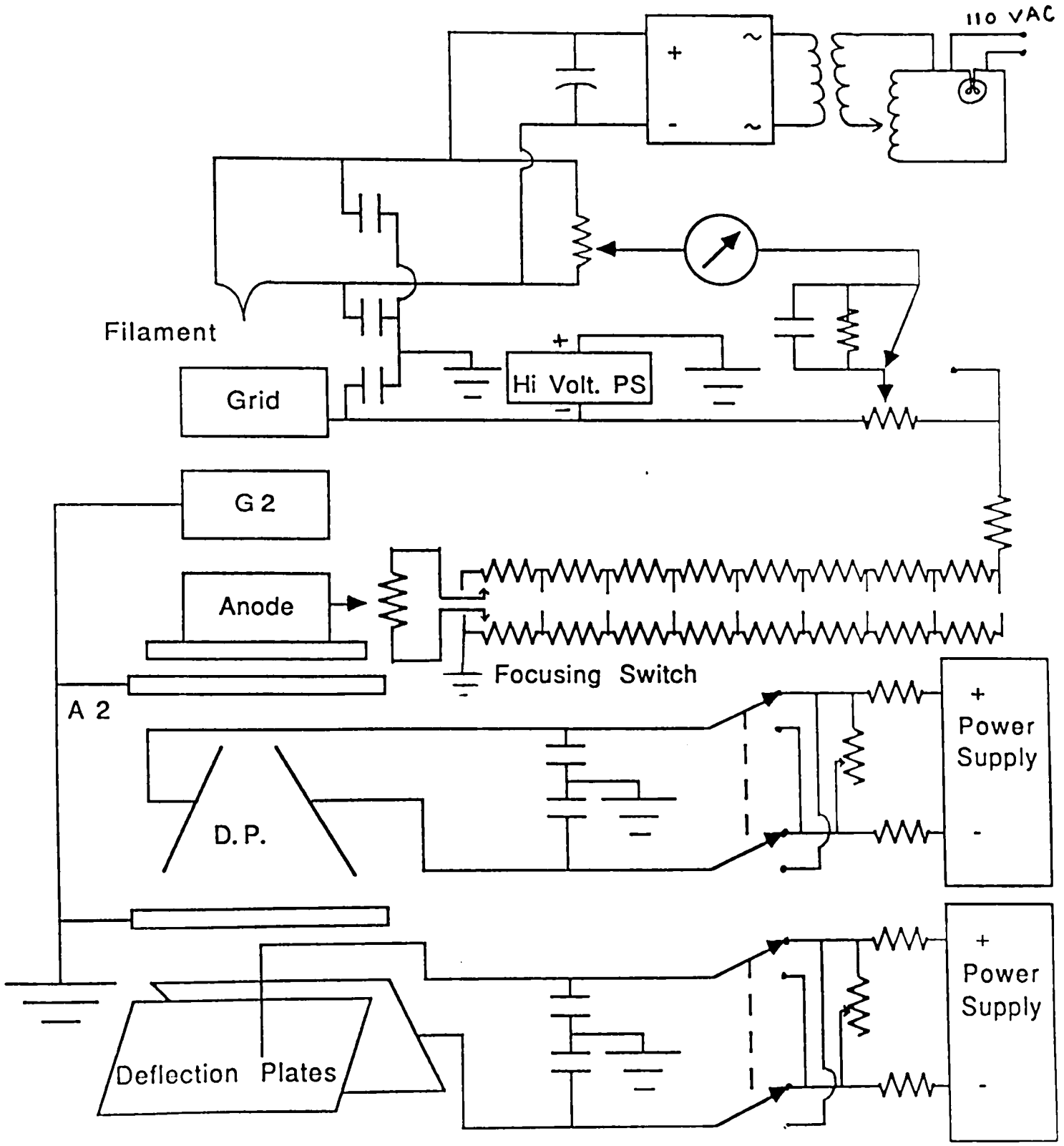

Figure 4.3: Schematic of the Electron Gun Control Circuits

batteries to the electrometer and to ground as shown in Figure 4.4. The electrometer used to measure the current is a Keithley 617 digital unit. Its analog output is connected to an Angus-Esterline x-y recorder to plot current vs. time. The dielectric sample surfaces charge very quickly, and the meter does not always record the rise in replacement current well. There is often a straight line with a large slope at the beginning of the curve indicating that the meter is trying to catch up to its input. This straight line forms a right triangle with the axes of the chart recorder. The time it takes to run a curve can be increased by using a lower beam current, or a thinner sample. The latest data were taken on thinner samples and with lower beam currents than the initial data.

After a set of sample runs, the samples are removed from the vacuum chamber, and each sample's capacitance is measured with a Tektronix Type 130 L-C meter. These values of capacitance are combined with the I_0 vs. t plots using Eqns. (3.7) and (3.8) to get δ vs. E_0 curves.

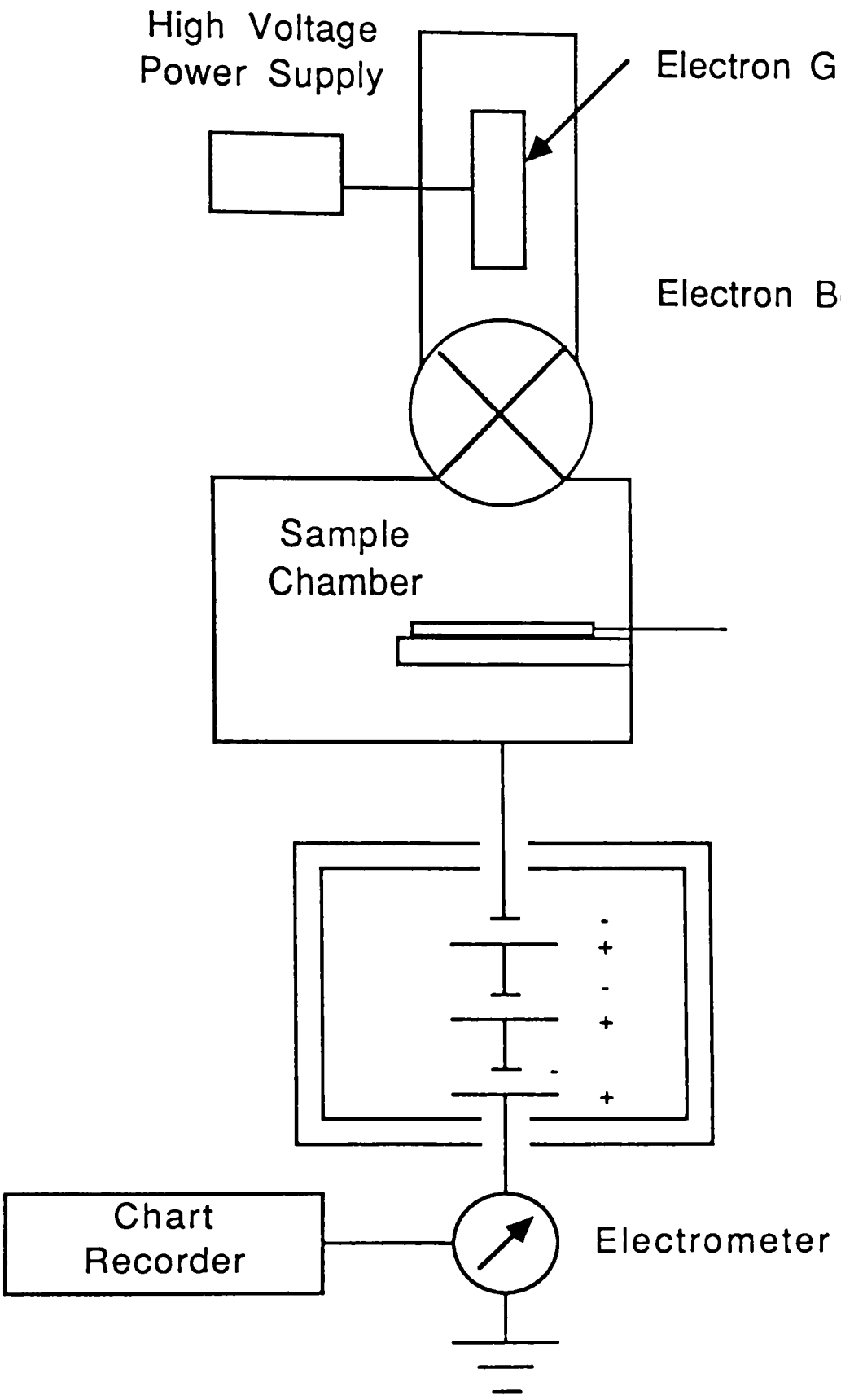

Figure 4.4: Schematic Representation of the Electrical Circuit

CHAPTER V

RESULTS

The raw data in this experiment are chart recordings of measured replacement current vs. time. The measured replacement current will include the actual replacement current, plus some leakage current due to a path from the bias batteries through the electrometer to ground. To find the leakage current, we measured the current through the electrometer with the bias batteries on, but the electron beam off, under normal vacuum conditions (1 to 4 $\times$ 10^{-7} Torr or less.) This leakage current value is subtracted from the measured replacement current to get the actual replacement current, I_0. On different days, the leakage current varied, possibly due to the humidity in the room. For measured replacement currents of about .17 nA, the leakage current was .008 to .023 nA (4.3% to 7.3%). The replacement current recorded was manually measured from the graph paper using constant time intervals, either .55 or .27 seconds, depending on the speed of the chart recorder during the run.

The list of replacement currents was entered into a computer program to calculate the effective energy, E_0, and δ at each point. Rectangular integration was used to obtain the energy, with a triangle in place of the first rectangle because the electrometer could not keep up with the true output at the beginning of each sample run. At each point, δ is calculated from the known beam current and actual replacement current:

$$I_0 = I_b - I_s \tag{5.1}$$

$$\delta = \frac{I_s}{I_b} \tag{5.2}$$

$$\delta = \frac{I_b - I_0}{I_b}. \tag{5.3}$$

The effective energy E_0 is calculated by approximating the integral in the E_0 equation by a summation:

$$E_0 = E_b - eV_s + \frac{e}{C}\int I_0 t$$

$$E_0 = E_b - eV_s + \frac{e}{C}\Sigma I_0 \Delta t,$$

where Δt is either .545 or .2725 seconds.

We tested Lexan (polycarbonate) and Lucite (PMMA) in this experiment. Some of the samples tested were virgin samples, just cut from bulk material and polished. Other samples were treated by coating them with a hydrocarbon material. The treated samples were prepared by Gary Leiker in the surface flashover laboratory at Texas Tech University.[1] These treated samples are first cut and polished like the virgin samples, but are then placed in a vacuum chamber and exposed to sparks from a jet engine sparkplug. This procedure gives the surface a thin (20-100 Angstroms) coating. This coating causes the high voltage flashover of the dielectrics to increase. The SEE data of these samples are studied to give information about the coating.

The battery voltage, V_0, was read just before the electron beam was turned on for a day's runs, Figure 5.1, (the batteries were turned on to stabilize for at least five hours before the experiment), and the voltage was read again after all the day's data were taken. Many times, the battery voltages before and after the samples were run differed by up to 8 volts, for some unknown reason. Figure 5.2 shows a raw data curve of I_0 vs. t from the chart recorder. (This particular curve is for a virgin Lucite sample.) After a list of $I_0(t)$ is measured from the raw data curve, the effective energy of the incident electrons and the SEEC are calculated and plotted by computer as shown in Figure 5.3. All of the curves for virgin materials exhibit similar behavior (rising to a maximum δ, then falling off), but curves of the same material did not line up. When we plotted δ vs. E_0 curves of the same material together, they did not align, they had different

[1] Leiker.

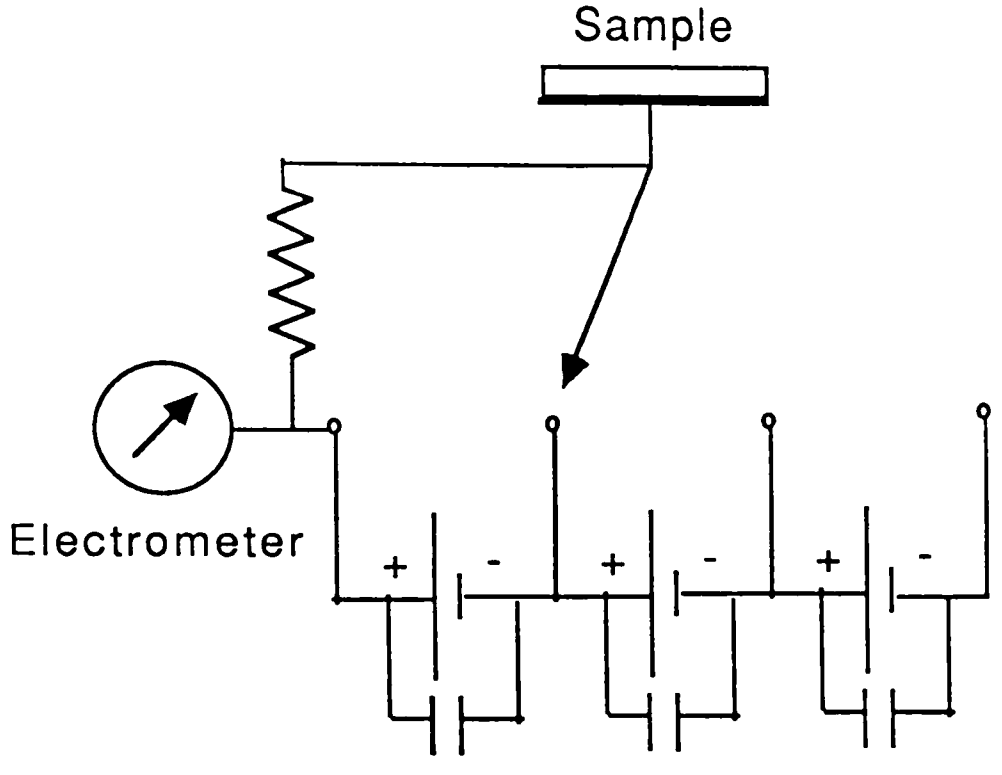

Figure 5.1: Measuring Circuit using Bias Batteries

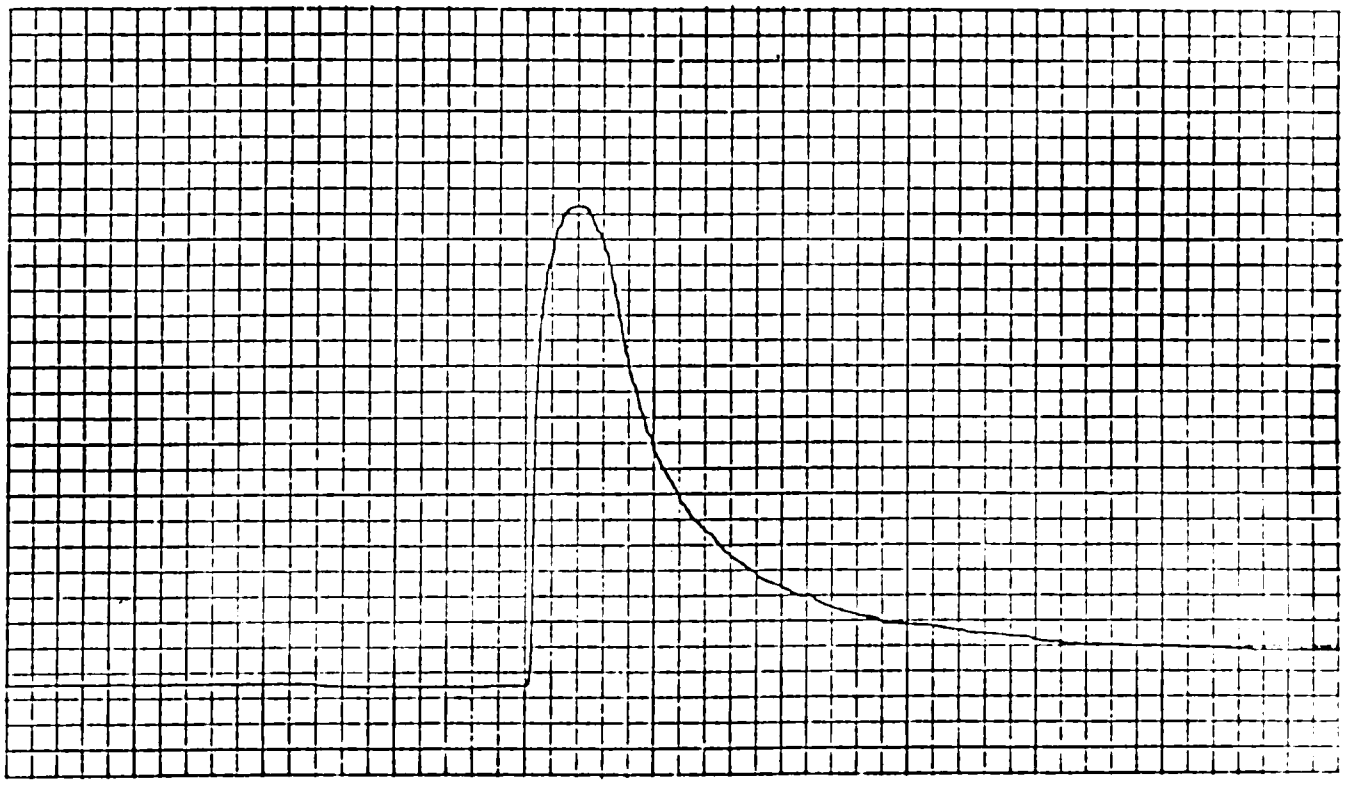

Figure 5.2: Raw Data Curve taken directly from Chart Recorder

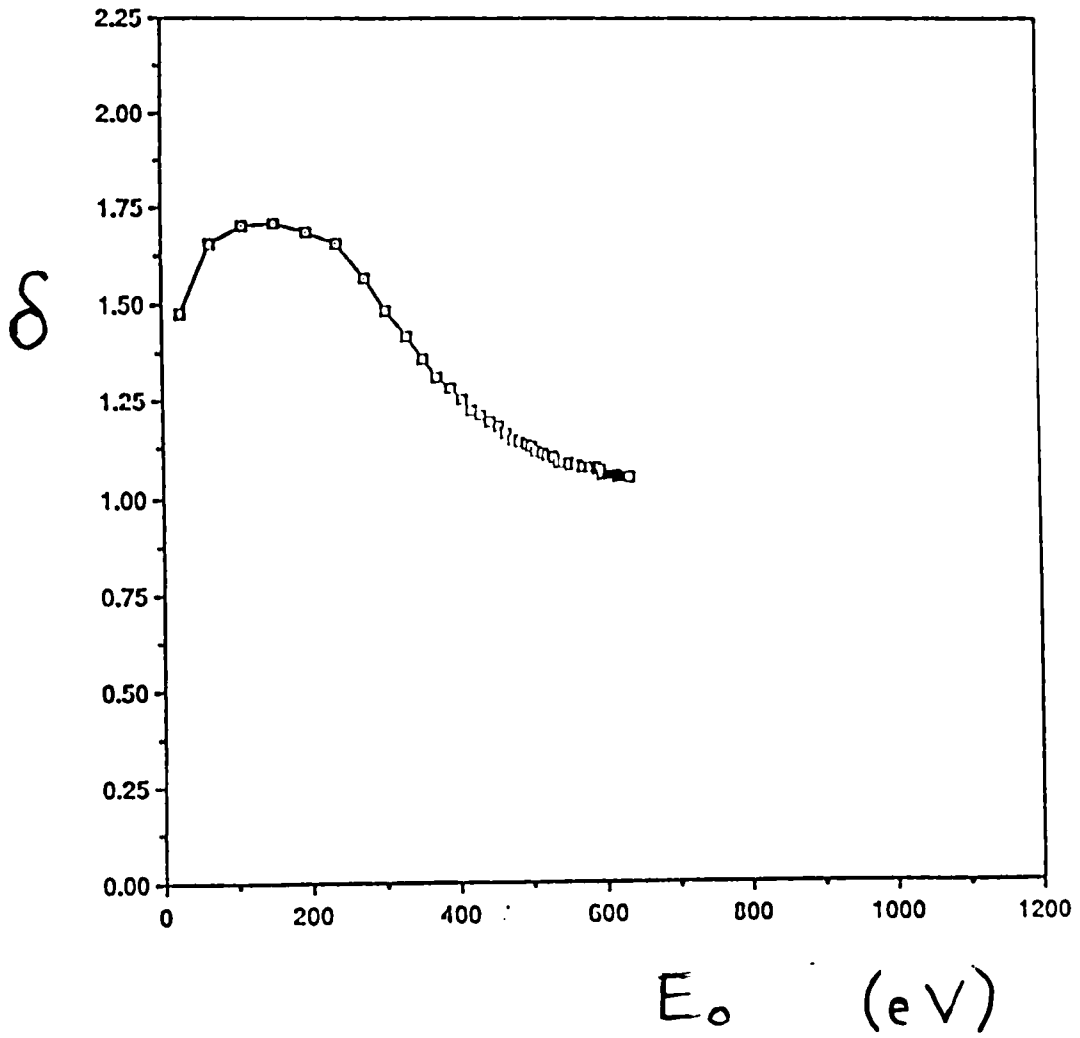

Figure 5.3: δ vs. E_o Plot (This Curve is for Lucite)

energies for their maximum δ. We hypothesized that we had a constant energy offset of unknown energy, so all of the curves for a given material were shifted linearly along the energy axis to have their peaks line up with the one curve for which we had the most confidence. Then we averaged all of the curves of that one material type together at specific energy values. These averages took away all shape of the curve, leaving a basically flat line. This means that we did not have a constant energy offset, but the energy we measured was incorrect by some non-linear function.

When universal curves are plotted, this problem disappears. Each data curve depends only on its own value of $E_{0,m}$, not on any other curves. All of the data taken were plotted as universal curves, and three distinct groups were found. Both virgin Lexan and virgin Lucite were found to follow the same universal curve, which we call our average universal curve for virgin polymers. This curve is shown in Figure 5.4. The error bars shown are for standard error, or standard deviation of the mean.

The second group of universal curves fits both all of the treated Lexan data, and the treated Lucite data taken in Fall, 1987. The average universal curve is shown in Figure 5.5, our treated polymer curve. For $\frac{E_0}{E_{0,m}} > 1$, this curve has a negative slope with a smaller absolute value than the slope for the virgin polymer curve.

The final group of data is the treated Lucite data taken in Summer, 1988. The coating on these samples did not display an SEEC curve similar to the previous treated Lucite samples. The average universal curve for these data, which we call unusual treated Lucite data, is shown in Figure 5.6. When all of these three average universal curves are plotted together, Figure 5.7, we see that the unusual Lucite results are well within the error bars of the virgin polymer curve. The coatings formed in the summer of 1988 appear to have no real effect on the secondary electron emission of Lucite, though the earlier coatings did. (The flashover response of these samples was not tested.) The discrepancy between these data and those of Fall, 1987, may be due to some difference in the way the coating was applied. By Summer 1988, Leiker's coating

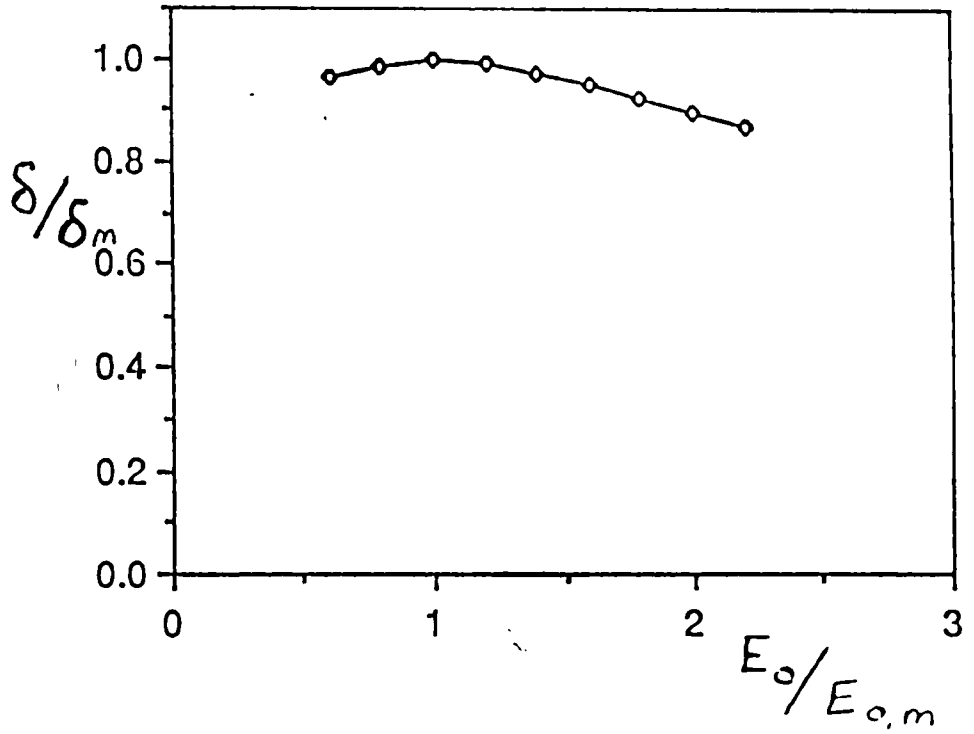

Figure 5.4: Average Universal Curve for Virgin Polymers

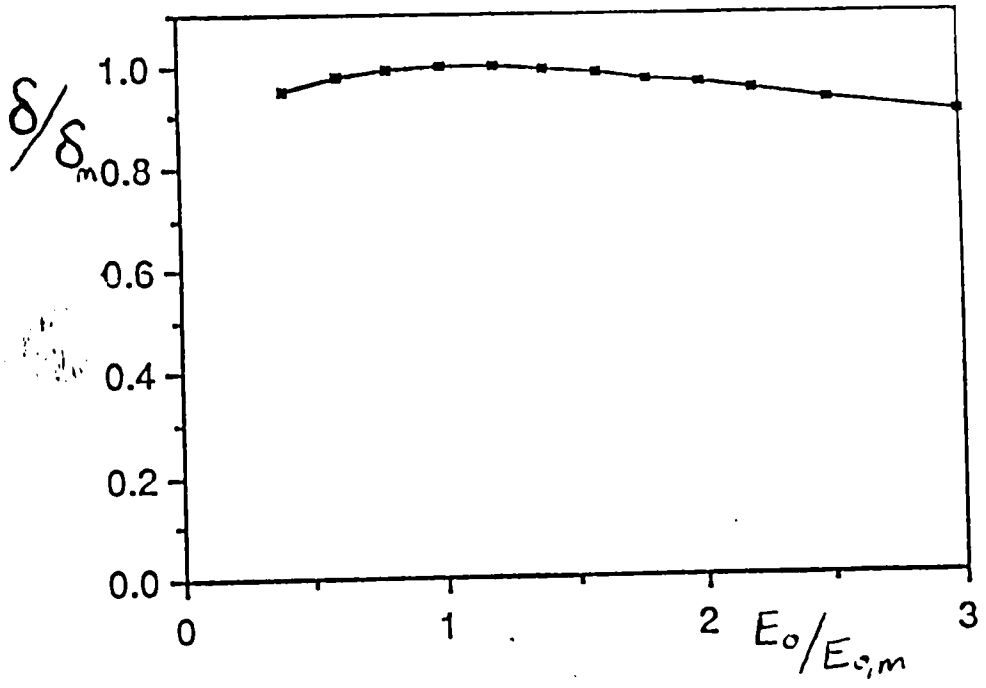

Figure 5.5: Average Universal Curve for Treated Polymers

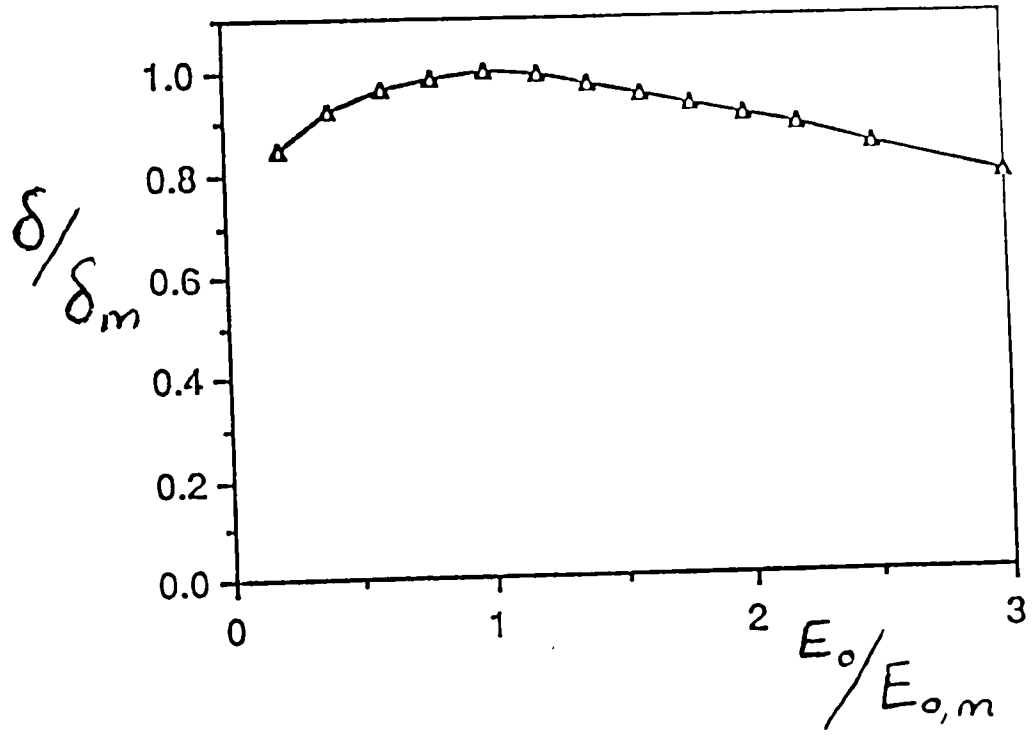

Figure 5.6: Average Universal Curve for Unusual Lucite Data

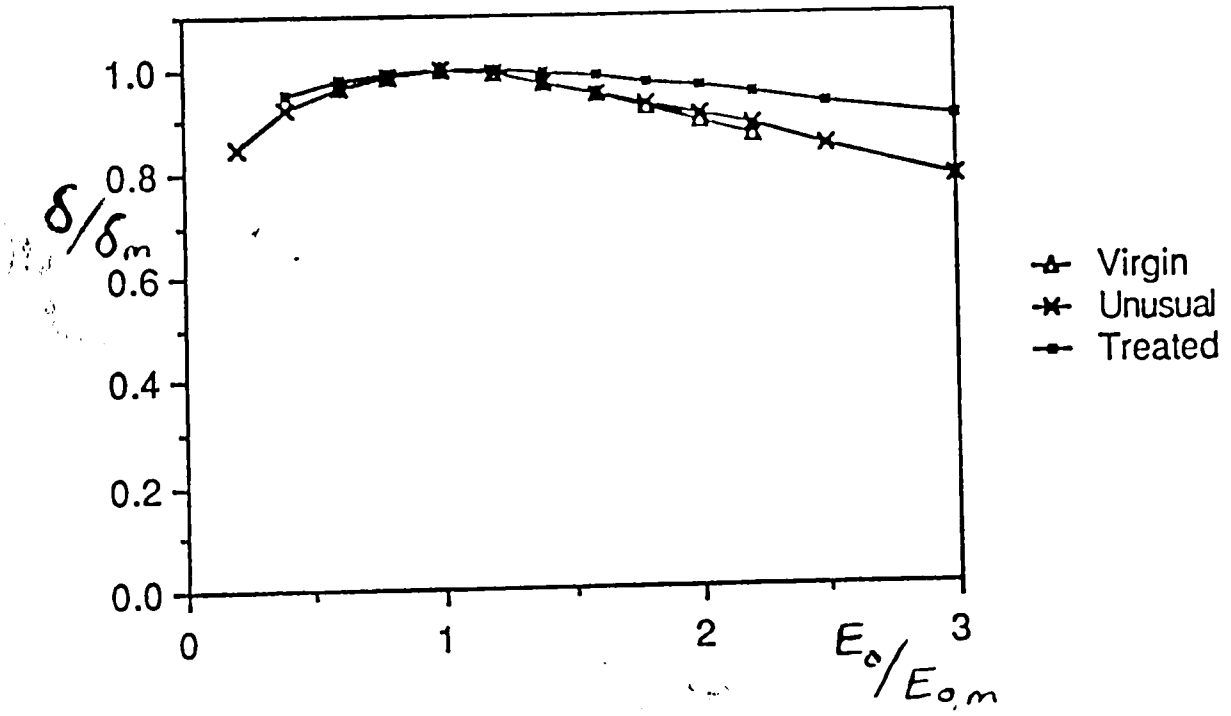

Figure 5.7: Average Universal Curves

apparatus and vacuum system had been shut down for several weeks. When the system was reactivated, the conditions may not have been the same as they were several months previously. Even if the coating conditions were similar, Lucite has always been a difficult material to get consistent results from, with regard to coating. Leiker found that some of his coated Lucite samples exhibited a consistent high flashover voltage, as did all of the treated Lexan samples, but some of the treated Lucite samples gave only one shot with a high flashover voltage, then had lower flashover voltages.[2] Baker[3] found that her treated Lexan samples were consistent with each other, but one of the treated Lucite samples had a curve similar to virgin Lucite, while the other had a curve similar to the treated Lexan. The way this hydrocarbon coating affects Lucite may be a key to understanding the coating.

In an effort to find what materials in the normal coating affect the SEEC, we also tested a Lexan sample, treated with a sparkplug with tungsten electrodes. Tungsten is one of the elements in the jet engine sparkplug used to coat the samples. A "sparkplug" was made with tungsten wire, and a sample of Lexan was coated using it. The δ vs. E_0 curve for the sample is shown in Figure 5.8. The universal curve for this tungsten coated Lexan sample, Figure 5.9 , shows a behavior between the behaviors of treated and virgin Lexan samples. This coating may be as thin as 20 Angstroms. At low energies, the incident electrons interact with the coating, but as their energies go up, the electrons have a higher probability of going through the coating and striking the Lexan underneath. So the low energy part of the curve shows the SEE of the coating, but at higher energies the curve drops off to approach a virgin Lexan SEE curve. More work is needed on coatings of different thicknesses and different substrates to see if this is actually what is happening.

---

[2] Leiker.
[3] Baker.

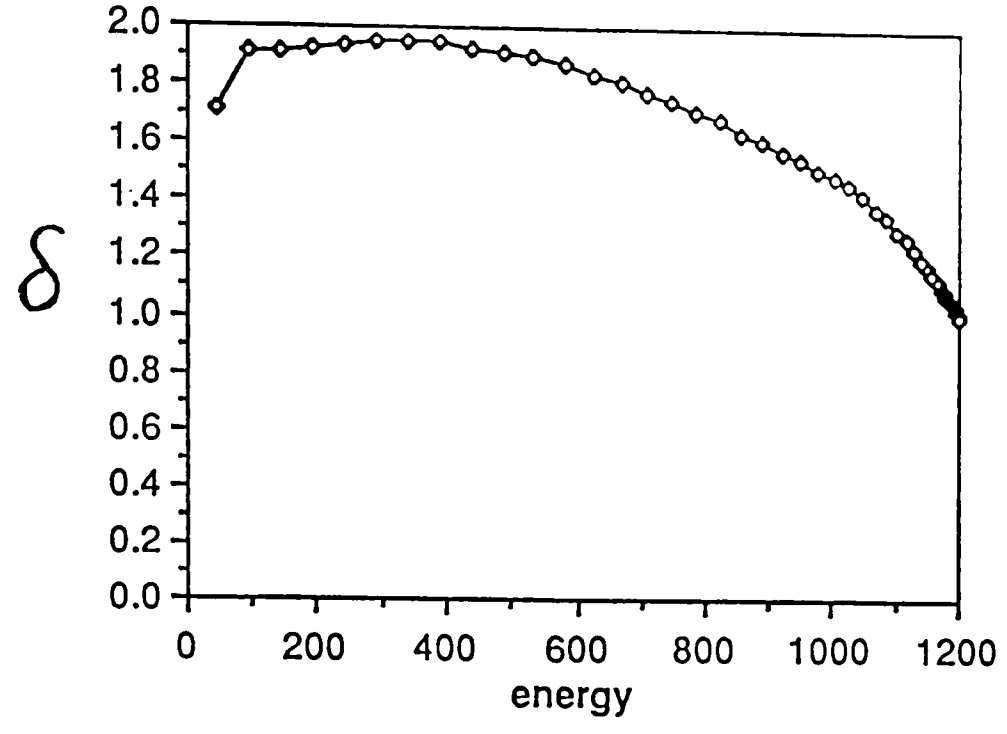

Figure 5.8: Tungsten Coated Lexan Data

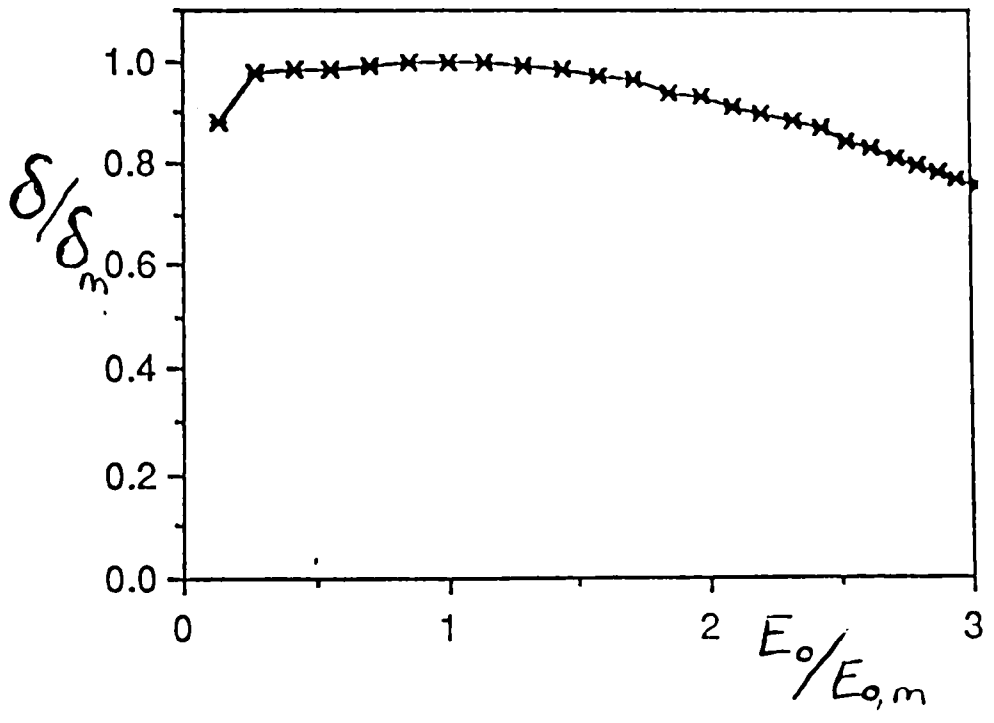

Figure 5.9: Universal Curve for Tungsten Coated Lexan

CHAPTER VI

CONCLUSIONS AND PROJECTIONS

To compare our results with some of the results in the literature, we want to find n for each type of universal curve, to fit in Burke's equation:

$$\delta = KE_0^{-n}. \tag{6.1}$$

We can plot $\ln(\frac{\delta}{\delta_m})$ vs. $\ln(\frac{E_0}{E_{0,m}})$, and the slope of the line will be $-n$. Our virgin polymer curve has $n = 0.65$. Our treated polymer curve has $n = 0.30$. Our universal curve for treated Lucite from Summer 1988, has $n = 0.61$. Willis and Skinner reported $n = 0.35$ for metals, semiconductors, and insulating solids. They also gave a value of $n = 1$ for polymers. Burke found $n = 0.725$ for polymers. All of their curves showed data from thin films, not bulk samples. The thin films were pure material, but our samples are bulk samples, cut from commercially available materials. The commercial materials have impurities added intentionally, such as antioxidants, plasticizers, and U-V retarders. The difference in sample purity should account for our n values being lower than those reported in the literature. Our values of n for treated samples suggest that the coating acts like a metal. The ESCA investigations, reported by Leiker,[1] found metal oxides on the surface of the treated samples.

Overall, we found δ_m's ranging from 1.4 to 2.1, but we were not able to determine $E_{0,1}$. On all of the δ vs. E_0 curves we have, we never got low enough in energy to reach the first crossover point, where $\delta = 1$. We expected that if we started with $E_0 < E_{0,1}$, the raw data curve of I_0 vs. t would show a negative spike because the surface would begin to charge negatively, instead of the usual positive peak and fall. We expected the first crossover point to be around 30 eV, but we

[1] Leiker, p. 53.

were apparently still above $E_{0,1}$ at 10 eV. It is possible that at these low energies our method for measuring the beam is inaccurate. The electron beam may be quite spread out, instead of being a narrow beam. For future work we need to design a gun to cover a smaller range of energies, at a lower voltage, so that we can know the energy more precisely, to be able to find the first crossover point.

We did have problems in knowing the energy of the incident beam. The battery voltage could vary up to 8 volts during one day's sample runs, and the cathode voltage set by the power supply could change by 3 volts, so the effective energy can only be known to an accuracy of 11 volts. The electron gun current changed significantly on a few of the runs, making the data questionable, so they had to be discarded. Probably a slight change in voltage from the AC regulator caused the fluctuation in the beam current, because the filament is very sensitive to the voltage across it. The effective energy could be wrong if the measured value of capacitance was incorrect, but this would be a non-linear error having a large effect at high energies, but only a very small effect at low energies, near the peak. Since we had problems with $E_{0,m}$'s not matching up for multiple samples, it is doubtful that an error in measuring the capacitance is to blame.

For further work to be done on this experiment, several improvements should be made. The electron gun should either be replaced, possibly with an SEM type gun, or at least the filament should be run from a regulated power supply, instead of an AC regulator and a rectifier to provide a more constant beam current. If tungsten filaments are used, as they have been here, then the small gate valve and the ion pump may be removed, because tungsten is not poisoned by the atmosphere when it is cool. Then the gun can be moved several inches closer to the sample so there is less distance for the beam to be affected by the earth's magnetic field or other stray fields caused by the equipment.

It is likely that larger diameter samples would work better, possibly with an evaporated guard ring on the back, like the ones used by Gross et al.[2] The sample holder should be completely redesigned to accomodate larger samples, or another method of charging, such as rastering across the sample with a tiny beam, and more accurate positioning of samples should be provided. Probably a rotary motion sample holder will work best to hold larger samples. Rastering allows us to know the exact size of the area covered by the electron beam. We could also be sure the beam does not come near the edge of the sample. (If the beam goes over the edge of the sample, it may strike the aluminum plate underneath, causing false replacement current readings.)

The way the samples are biased must be changed to improve the data. The batteries should be replaced by a well regulated, variable output power supply. It may be possible to change the bias as the sample is being charged, to slow the rise in replacement current on the output curve. As the beam strikes the sample, we make the sample bias more negative, down to a constant bias. The measured replacement current would be a function of the true replacement current and the system biasing, so the true replacement current could be deconvoluted out of the measured replacement current. Even if this changing bias is not used, the output of the electrometer should be fed to a computer to automatically integrate the δ vs. E_0 curve, to take out the human error involved in measuring currents off the chart recording.

There may be a better characterized material to use for calibrating the gun than graphite. A more extensive literature search should provide the best material, whose δ values are well known at both low and high energies. We do know that the graphite we use can become contaminated by substances in the chamber, probably diffusion pump oil. We need to find a calibration material which can be easily cleaned each time samples are replaced.

---

[2]Gross, von Seggern, and Berraissoul.

It also may be a good idea to pulse the beam on and off and use the charge measuring ability of the electrometer. The charge could be read by the electrometer after each current pulse. This would remove the error of measuring I_0 off the graph when integrating to find E_0. But any leakage current in the circuit will affect this measuring method.

Even without any of these additional improvements, the present apparatus and method allow the measurement of SEE curves for bulk samples of dielectrics. It is hoped that all future work will give more accurate results and determine the energies of the first crossover points for various materials.

REFERENCES

[1] Baker, M. C., Master's Thesis, Texas Tech University, 1985.

[2] Baroody, E. M., "A Theory of Secondary Electron Emission from Metals," Physical Review *78* (1950), pp. 780-787.

[3] Bruining, H., *Physics and Applications of Secondary Electron Emission* (New York: McGraw-Hill, 1954).

[4] Burke, E. A., "Secondary Emission From Polymers," IEEE Transactions on Nuclear Science *NS-27* (1980), pp. 1760-64.

[5] Dekker, A. J., "Secondary Electron Emission," Solid State Physics *6* (1958), pp. 251-311.

[6] Dekker, A. J., *Solid State Physics* (Englewood Cliffs, N. J.: Prentice- Hall, 1957), p. 420.

[7] Gross, B., H. von Seggern, and A. Berraissoul, "Surface Charging of Dielectrics by Secondary Emission and the Determination of Emission Yield," IEEE Transactions on Electrical Insulation *EI-22* (1987), pp. 23-28.

[8] Gross, B., H. von Seggern, J. E. West, "Positive Charging of Fluorinated Ethylene Propylene Copolymer (Teflon) by Irradiation with Low-energy Electrons," Journal of Applied Physics *56* (1984), pp. 2333-2336.

[9] Kazantsev, A. P., and T. L. Matskevich, "Secondary Electron Emission of Methylmethacrylate at 25 keV," Soviet Physics-Solid State *6* (1965), pp. 1898-1904.

[10] Leiker, G. R., Ph. D. Dissertation, Texas Tech University, 1988.

[11] Matskevich, T. L., "Secondary Electron Emission of Some Polymers," Fizika Tverdogo Tela, Collected Papers, *1* (1959), pp. 277-279.

[12] Matskevich, T. L., and E. G. Mikhailova, "Secondary Electron Emission in Ice and Anthracene Films," Soviet Physics-Solid State *2* (1960), pp. 655-659.

[13] von Seggern, H., "Charging Dynamics of Dielectrics Irradiated by Low- Energy Electrons," IEEE Transactions on Nuclear Science *NS-32* (1985), pp. 1503-1511.

[14] Whetten, N. R., "Secondary Electron Emission of Vacuum-Cleaved Solids," Journal of Vacuum Science & Technology *2* (1965), pp. 84-86.

[15] Willis, R. F., and D. K. Skinner, "Secondary Electron Emission Yield Behavior of Polymers," Solid State Communications *13* (1973), pp. 685-688.

PERMISSION TO COPY

In presenting this thesis in partial fulfillment of the requirements for a master's degree at Texas Tech University, I agree that the Library and my major department shall make it freely available for research purposes. Permission to copy this thesis for scholarly purposes may be granted by the Director of the Library or my major professor. It is understood that any copying or publication of this thesis for financial gain shall not be allowed without my further written permission and that any user may be liable for copyright infringement.

Disagree (Permission not granted)	Agree (Permission granted)
_____	Elise Bornmann
Student's signature	Student's signature
_____	12-14-88
Date	Date